X-ray tomography, digital volume correlation and FE modelling: A synergistic combination to study the processing-structure-property relations in ductile iron

Andriollo, T.; Zhang, Y.; Fæster, S.; Thorborg, J.; Tiedje, N. S. ; Kouznetsova, V.; Hattel, J.

Published in:
IOP Conference Series: Materials Science and Engineering

Link to article, DOI:
10.1088/1757-899X/861/1/012037

Publication date:
2020

Document Version
Publisher's PDF, also known as Version of record

X-ray tomography, digital volume correlation and FE modelling: A synergistic combination to study the processing-structure-property relations in ductile iron

IOP Conf. Series: Materials Science and Engineering **861** (2020) 012037 doi:10.1088/1757-899X/861/1/012037

X-ray tomography, digital volume correlation and FE modelling: A synergistic combination to study the processing-structure-property relations in ductile iron

T Andriollo[1], Y Zhang[1], S Fæster[1], J Thorborg[1,2], N S Tiedje[1], V Kouznetsova[3] and J Hattel[1]
[1] Technical University of Denmark, Kgs. Lyngby, Denmark
[2] MAGMA GmbH, Aachen, Germany
[3] Eindhoven University of Technology, Eindhoven, The Netherlands

E-mail: titoan@mek.dtu.dk

Abstract. The mechanistic understanding of the processing-structure-property relations in ductile iron is still far from complete. One reason is that the impact on the mechanical properties of some of the microstructural features arising from the casting process can be hard or even impossible to investigate using experimental methods alone. The present work shows that a solution can be the synergistic combination of X-ray tomography, digital volume correlation (DVC) and finite element modelling, which are applied here to study the effect played by the Si micro-segregation and local residual stresses upon mechanical loading. First, miniaturized tensile and compact tension specimen are loaded incrementally while imaging with X-ray tomography. Then, the micro-scale displacement is reconstructed with DVC and used to prescribe the boundary conditions in high-fidelity 3D finite element models of the microstructure. Simulations are run considering or not the formation of the local residual stresses and build-up of micro-segregation during manufacturing. The numerical predictions are compared to the corresponding experimental data both at the macro-scale – applied load – and at the micro-scale – strain field reconstructed with DVC. This allows for a first assessment of the impact of the local residual stresses and Si micro-segregation on the mechanism of tensile deformation as well as of crack propagation of ductile iron.

1. Introduction

Since its commercial introduction in 1948, ductile iron, also known as nodular cast iron or spheroidal graphite iron (SGI), has constantly found new fields of application, ranging from the automotive sector to the wind power industry. Nowadays, this positive trend is challenged by the limitations in terms of reliability and range of applicability of the processing-microstructure-property relations available in the literature, which are rooted in the still incomplete understanding of the mechanisms controlling deformation and fracture at the microscale [1]. This is primarily a consequence of the complex material microstructure, composed of graphite nodules embedded in a matrix where multiple phases may coexist depending on chemistry and cooling conditions, which makes direct experimental investigations challenging.

In this respect, a breakthrough in the experimental characterization of SGI has been achieved in the last 10-15 years with the introduction of techniques based on X-ray computed tomography (CT), which have been applied to visualize the microstructure evolution in 3D during both manufacturing

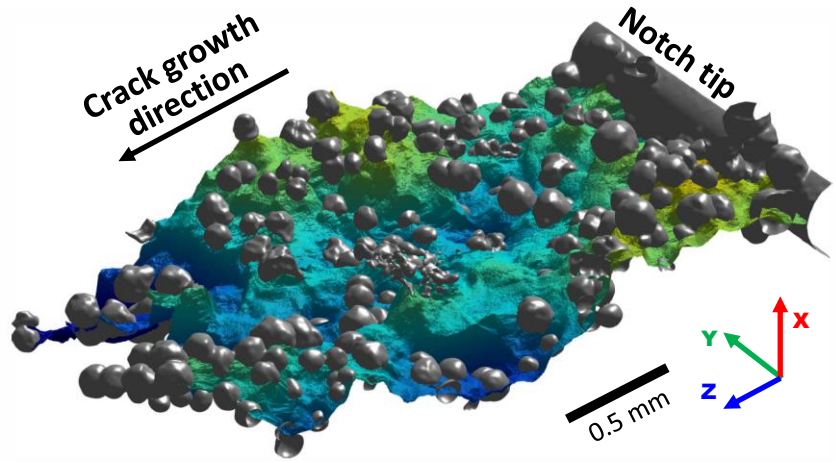

Figure 1. Fatigue crack path at the microstructural scale in a 1.5 mm thick compact tension specimen, reconstructed from CT via a dedicated segmentation procedure. Adapted from [2].

and room temperature mechanical loading [3, 4]. A great advantage of CT is that it can be combined with pattern tracking methods like digital volume correlation (DVC) and used to reconstruct the deformation field at the level of the microstructure during both monotonic [5] and cyclic loading [6]. This has opened up to the possibility to observe and quantify the interaction between the microstructural constituents with unprecedented level of detail. An example is given in figure 1, where a 3D reconstruction of a fatigue crack which grows by linking the nodules in a 1.5 mm thick compact tension specimen is depicted.

In spite of these powerful experimental techniques, some aspects of the deformation of SGI at the microscale remain challenging to investigate. Among these is the impact of those microstructural factors whose individual effects are hard or even impossible to isolate because of experimental difficulties in changing such factors without changing, at the same time, other important microstructural parameters. The Si micro-segregation and the local residual stresses are two examples of these. The former builds up during solidification due to the progressive decrease in Si content of the liquid combined with the Si rejection from the growing graphite, whereas the latter form during solid-state cooling due to the thermal contraction mismatch between the nodules and the matrix. Recent work pointed out that the local residual stresses can reach magnitudes of 100 – 150 MPa [7, 8]. At the same time, extensive Si micro-segregation [9] can be expected to produce localized variations of the matrix yield stress in the order of 50 – 100 MPa [10]. When these values are compared to the macroscopic yield stress of standard SGI grades, it is clear that both factors can potentially play a significant role in how the material behaves upon mechanical loading.

Recently, the authors introduced a framework based on the synergistic combination of CT, DVC and finite element (FE) modelling to predict the yield stress [11] and the fatigue crack growth direction [2] in SGI. In this work, the Si micro-segregation and local residual stresses are taken as test cases to demonstrate that the same framework can be used to study the impact of the microstructural factors that, for the reason stated above, are hard to investigate with experimental methods alone.

2. Methodology

The framework laid out in [2, 11] is summarized briefly in the following subsection. Next, the modifications needed to include the impact of the Si micro-segregation in the FE models are described. It is worth noting that the formation of the local residual stresses was already taken into account in the works [2, 11]. However, the associated effects were investigated in relation to the SGI yield stress only, not with respect to the crack propagation direction at the microscale.

2.1. Overall framework

The overall idea of the framework described in ref. [2, 11] is to perform a mechanical test on a miniaturized specimen while imaging in-situ with CT. Based on the CT data, the micro-scale displacement is reconstructed with DVC [12] and used to prescribe the boundary conditions in a 3D microstructure-resolved FE model of the region of interest. This approach offers two main advantages. First, the size of the model can be maintained small compared to that of the specimen, meaning that the computational complexity can be kept at a reasonable level. Second, the numerical predictions can be compared to the corresponding experimental data both at the macro-scale and at the micro-scale in a combined fashion.

The specific mechanical test considered in [11] is a uniaxial tensile test, conducted on a mainly ferritic SGIs with a small fraction of pearlite ≈ 5% and highly spherical nodules. The left-hand side of figure 2 shows the specimen and the associated FE model. In the model, which corresponds to the region of the specimen between two cross-sections, the subdivision of the microstructure into matrix and nodules is taken into account based on the information from the CT. The matrix is assumed to obey an isotropic elastoplastic constitutive model with isotropic hardening, whose parameters are calibrated using experimental data of an alloy with equivalent metallurgical parameters. The nodules are assumed linear elastic and their highly inhomogeneous internal structure is modelled by dividing each nodule into an external shell and a core. While the former is assumed isotropic, different orientations of the elastic symmetry and anisotropic moduli are assigned to each mesh element in the core based on the element location with respect to the centroid of the nodule, in order to represent, approximately, the strong gradient in mechanical properties inside the nodules [13, 14]. The weak interface between the nodules and the matrix is modelled using the surface-based cohesive formulation available in ABAQUS to allow for interface debonding. The model is subjected to two simulation steps. First, to simulate the formation of the local residual stresses, the last part of the solid-state cooling is simulated by prescribing a uniform temperature change from 500 ºC to 20 ºC. Then, the displacement reconstructed with DVC is prescribed on the model boundaries to simulate the tensile testing. Further details can be found in [11].

Conversely, the mechanical test considered in [2] is a fatigue crack growth test. The right-hand side of figure 2 shows the compact specimen used in the test and the associated crack tip FE model. In this case, the region considered in the model is the volume surrounding the crack tip. Besides an internal

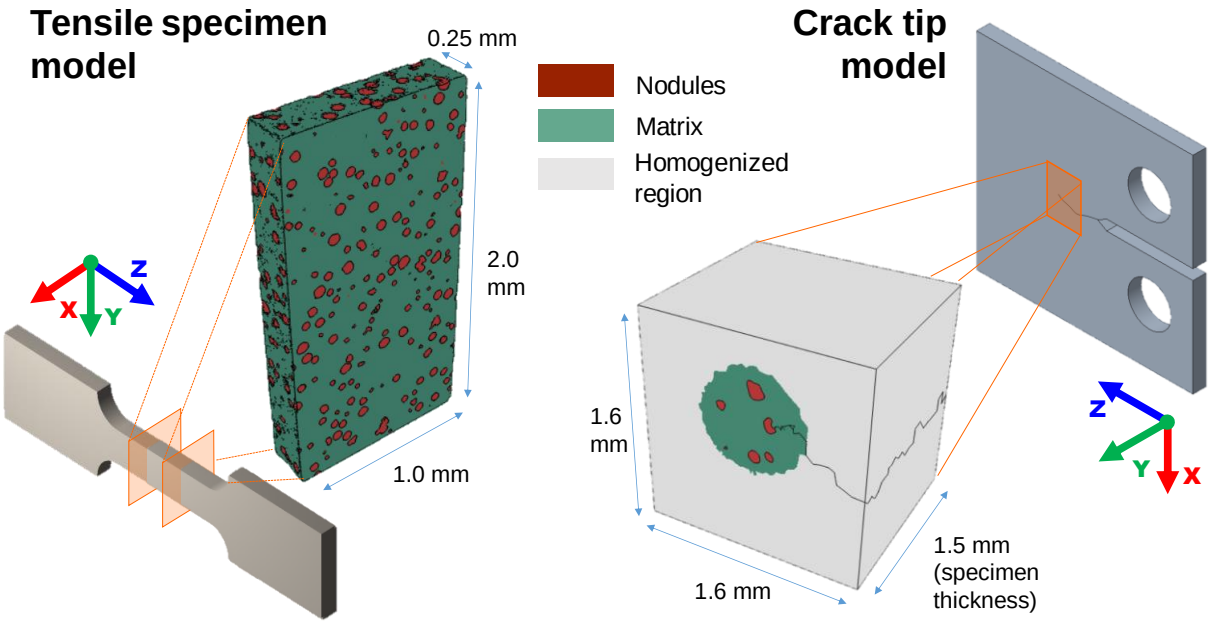

Figure 2. Miniaturized tensile and compact tension specimens and corresponding FE models.

microstructure-resolved region, the model features an additional external homogenized region, whose purpose is to transfer the load to the internal region in a more gradual fashion, as well as a stationary crack, which is inserted in the model based on the real crack geometry reconstructed with CT (shown in figure 1). The constitutive behaviour of the nodules and of the nodule-matrix interface is equivalent to that described in relation to the tensile specimen model. Conversely, an isotropic elastoplastic formulation with both isotropic and kinematic hardening is selected for the matrix, whose parameters are calibrated by constructing a representative volume element of the microstructure and fitting its macroscopic response – computed via first-order computational homogenization [15] – to cyclic experimental data for the considered SGI. The homogenized region obeys the same constitutive model of the matrix, although with a different set of parameters, chosen to represent the SGI effective behaviour. The solid-state cooling is simulated as in the tensile specimen model. Subsequently, five consecutive loading cycles with identical boundary conditions (prescribed boundary displacement at maximum and minimum load on the model boundaries) are simulated, in order to achieve stabilization of the micromechanical fields, i.e. hardening. Further details about this model can be found in [2].

2.2. Si micro-segregation

The micro-segregation of Si in the SGI microstructure is primarily a consequence of the positive Si partition coefficient in temperature range of the stable and metastable eutectic, which causes the Si content in the liquid to decrease progressively as solidification proceeds [16]. As the diffusivity of Si in the solid is limited, the room-temperature microstructure exhibits first-to-solidify regions characterized by a Si content larger than the average, and last-to-solidify regions where the Si content is significantly lower. On top of this, the Si rejection by the growing graphite plays a role also and tends to increase the Si concentration near the nodules.

The above arguments indicate that if a high-resolution 3D map of the Si content is not available, the Si segregation pattern can still be estimated based on the location of the first-to-solidify and last-to-solidify regions and on the spatial distribution of the graphite. The latter can be easily obtained with CT, whereas the former necessitates laborious procedures based on serial sectioning to be determined.

In the present work, since the 3D subdivision of the microstructure into first-to-solidify and last-to-solidify regions could not be determined, it was decided to estimate the Si segregation pattern based on the distribution of the graphite nodules only. Specifically, it was assumed that the Si concentration w at a given point in the matrix is a decreasing function of the distance r to the closest nodule, which can be computed by applying a distance transform algorithm to the segmented CT images. Despite this assumption might appear simplistic, it is remarked that since the nodules in the last-to-solidify regions are smaller and usually more distant from each other than those in the first-to-solidify regions, a lower Si concentration is estimated in the former regions than in the latter, in agreement with experimental findings.

In the matrix region of both the tensile specimen and crack tip models the Si concentration was prescribed according to the following function:

$$\begin{cases} w(r) = w_{max} - \dfrac{w_{max} - w_{min}}{r^*} r & \text{if } r \le r^* \\ w(r) = w_{min} & \text{if } r > r^* \end{cases} \tag{1}$$

where w_{max} is the concentration at the nodule-matrix interface and w_{min} the minimum concentration found in the last-to-solidify regions. The threshold r^* was introduced in order to avoid having an extremely low concentration in some remote areas (e.g. the corners of the model) and it was adjusted so that the volume satisfying $r > r^*$ was no more than 1 % of the total matrix volume. The values of w_{max} and w_{min} were set to 2.75 wt% and to 1.50 wt%, respectively, based on previous segregation studies [17,18] and on the requirement of having an average Si concentration w_{avg} equal to that of the SGI used for manufacturing the tensile and compact tension specimens (2.30 %). Figure 3 shows the Si concentration prescribed according to equation (1) over the central X-Y cross-section of the tensile specimen model.

In the FE models, the Si micro-segregation was assumed to affect the local yield stress of the matrix σ_y. Specifically, the following Voce-type relationship was assumed to apply:

$$\sigma_y = Q^0 + Q^\infty(1 - \exp(-b\varepsilon^{pl}_{eq})) \quad (2)$$

where ε^{pl}_{eq} is the equivalent plastic strain, b is a constant and the parameters Q^0 and Q^∞ depend linearly on the local Si concentration:

$$\begin{aligned} Q^0 &= Q^0_{avg} + k^0(w - w_{avg}) \\ Q^\infty &= Q^\infty_{avg} + k^\infty(w - w_{avg}) \end{aligned} \quad (3)$$

The proportionality factors k^0 and k^∞ were set to 57.9 MPa/wt% and 76.2 MPa/wt%, respectively [10].

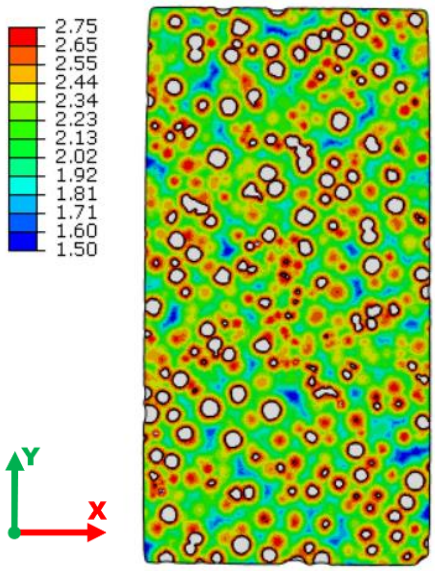

Figure 3. Si concentration over the central X-Y cross-section of the tensile specimen model. Values are in wt%. White areas represent the nodules.

3. Results

3.1. Monotonic tensile deformation

The model of the tensile specimen shown in figure 2 was used to simulate the deformation of the SGI microstructure upon tensile loading up to a macroscopic strain of 3.8 %. The nodal reaction forces on the Z+ boundary were recorded at regular intervals and used to compute the macroscopic tensile stress. The results are shown in figure 4 and relate to two simulations: one assumes uniform Si concentration whereas the other considers the Si segregation pattern described by equation (1). Hardly any changes in the predicted stress vs. strain curve can be detected when the Si segregation pattern is included in the FE model. That is, the non-uniform spatial distribution of the matrix properties does not seem to play a role. It is worth remarking that, as the average Si concentration is the same in both simulations, the average volumetric yield stress and strength of the matrix are also the same due to the linearity of equations (1) and (3). To a certain degree, this can explain why the macroscopic response of the SGI as predicted by the FE model is unaffected by the presence of Si segregation.

In order to investigate the deformation at the level of the microstructure, the predictions of the FE model were compared to the data from DVC. As discussed in [11], the comparison is not straightforward when a subvolume-based DVC algorithm is employed, due to the different locations at which the displacement vector is known, i.e. at the centre of each subvolume in DVC but at each node in the FE model. In the present work, as the FE mesh is much finer than the subvolume grid used in the DVC, it was decided to make the comparison at the level of the DVC grid. Accordingly, the displacement of each DVC subvolume, as predicted by the model, was considered equal to the mean displacement of all the FE nodes located inside that subvolume. Based on this "averaged" displacement, the equivalent strain predicted

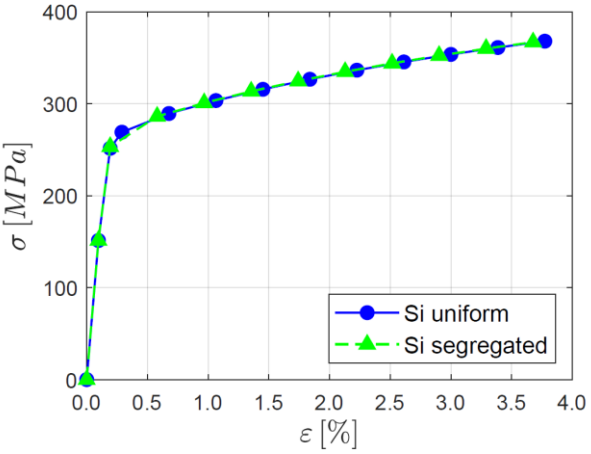

Figure 4. Tensile curves predicted by the FE model of the tensile specimen.

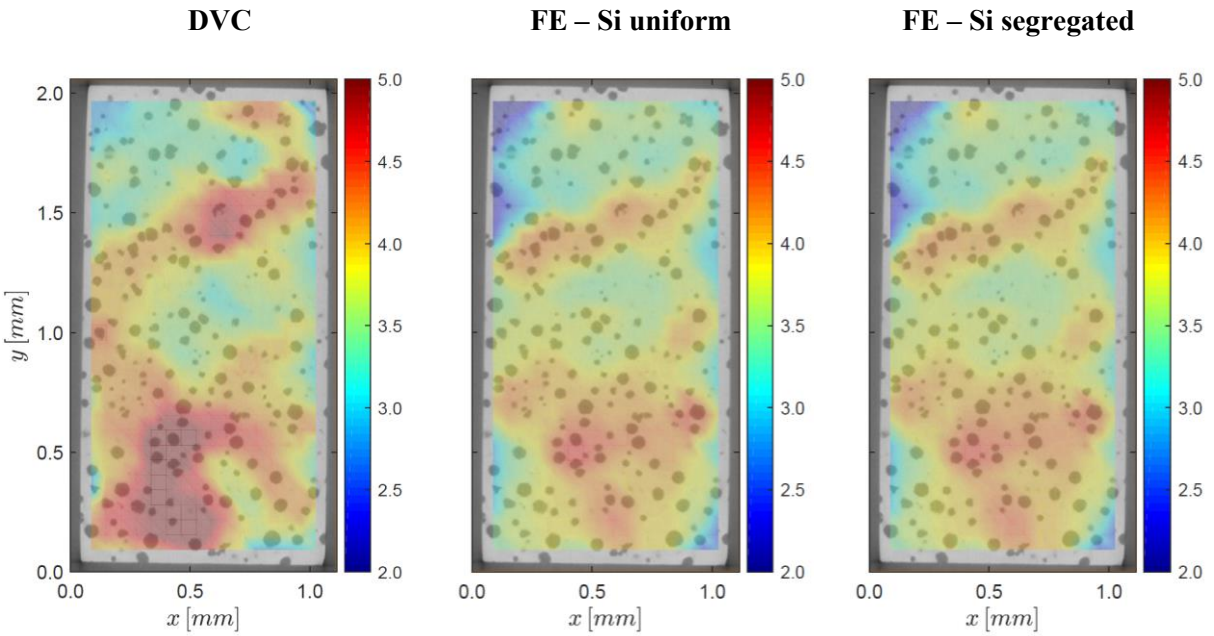

Figure 5. Contours of the equivalent strain (in %) over the central cross-section of the tensile specimen, superimposed onto the CT scan. The data relates to a macroscopic strain of 3.8 %.

by the model at the level of the microstructure was calculated and compared with the corresponding DVC data.

The comparison is shown in figure 5 for the central cross-section of the tensile specimen, where, as before, the predictions of two simulations which either account or not for the Si segregation are considered. Focusing on the DVC strain data, it can be observed that the deformation pattern seems to follow the underlying distribution of the nodules. The FE model that assumes uniform Si concentration can reproduce this pattern relatively well, even though some non-negligible differences exist (see e.g. the area near the bottom left corner of the cross-section, which is highly strained according to the DVC but not according to the FE simulation). Including the Si segregation in the FE model leads to negligible changes in the predicted strain values and, consequently, the agreement with the DVC data does not improve. In this respect, it is worth emphasizing that recent experimental studies demonstrate that the subdivision of the SGI matrix into first-to-solidify and last-to-solidify regions and the resulting spatial variation in mechanical properties do have an impact on how the material deforms at the level of the microstructure [19]. A possible explanation for why this effect is not seen in the present FE simulations is that, in addition to the Si segregation, there are other metallurgical factors that contribute to create a difference between the mechanical properties of the matrix in the former regions, which are not taken into account in the present model, e.g. porosities, grain size, pearlite fraction, etc.

3.2. Fatigue crack propagation

The model of the fatigue crack tip illustrated in figure 2 was used in [2] to show that the crack growth direction at the microstructural level correlates well with the direction perpendicular to the maximum principal stress predicted in the matrix. In the present work, the same model was used to investigate the extent to which the crack growth direction can be affected by the magnitude of the local residual stresses and by the Si segregation, which was neglected in [2]. To this end, four FE simulations were run, each corresponding to a different combination of the initial stress state (with/without residual stresses) and Si concentration pattern (uniform/segregated according to equation (1)). The output of each simulation was used to predict the crack growth angle in the X-Z plane (see figure 2) at 500

points along the crack front, based on the maximum principal stress direction. Subsequently, the difference $\Delta\theta_{ZX}$ with the propagation angle measured with CT upon reloading of the compact tension specimen was computed.

The results are presented in figure 6 in the form of box plots, where the horizontal band in each box indicates the median of the $\Delta\theta_{ZX}$ values along the crack front, the box edges represent the 25th and the 75th percentile and the whiskers extend to cover a length of 2.7 times the standard deviation. It can be seen that the four simulations give rise to almost identical box plots, which indicate, based on the position of the box edges, that the absolute value of $\Delta\theta_{ZX}$ is less than ≈ 10 degrees for 50 % of the points considered along the crack front. That is, there is good agreement between the predicted and the measured crack propagation angles independently of the simulation type. Consequently, the local residual stresses and the Si segregation do not appear to affect the crack propagation at the microstructural level significantly.

This result can be partially justified as follows. It is experimentally documented that the fatigue crack grows by linking the nodules, which tend to be approached by the crack along their radial direction. As the crack propagates perpendicularly to the maximum principal stress, it follows that the latter is roughly perpendicular to the nodule radius. Now, focusing on a single nodule, the local residual stresses around it can be considered spherically symmetric to a first approximation, and are such that any direction perpendicular to the nodule radius is a direction of maximum principal stress. Therefore, the local residual stresses and the actual stresses that drive the crack growth share the direction of the maximum principal stress. Therefore, a lower or a higher magnitude of the residual stresses cannot be expected to change significantly the resulting maximum principal stress direction and, therefore, the crack propagation direction. A similar reasoning might hold for the Si segregation pattern, given its approximate spherical symmetry near each nodule, see equation (1).

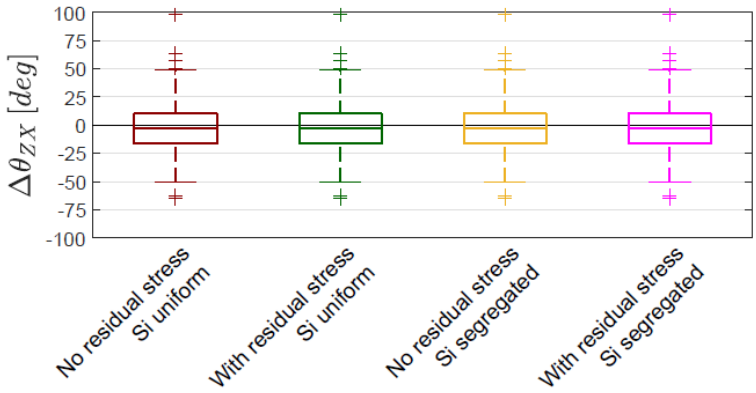

Figure 6. Statistical box plots of the angle $\Delta\theta_{ZX}$ between the predicted and the measured fatigue crack propagation directions at 500 points along the crack front.

4. Conclusions

The synergistic combination of CT, DVC and FE modelling allows developing computationally tractable microstructure-resolved thermo-mechanical models of SGI that can be validated at both the macro- and micro-scale. This opens up to the possibility of analysing the impact of some of those microstructural factors that are difficult to investigate with experimental methods alone. In this respect, it was shown here that the Si micro-segregation is not expected to affect significantly the material tensile response, either at the micro- or at the macro-scale, under the assumption that the Si concentration is a function of the distance to the closest graphite particle. The fatigue crack propagation direction in the matrix, computed based on the maximum principal stress direction, turned out to be unaffected by both the Si segregation and the local residual stresses forming during the solid-state cooling.

References

[1] Hütter G, Zybell L and Kuna M 2015 Micromechanisms of fracture in nodular cast iron: From experimental findings towards modeling strategies – A review *Eng. Fract. Mech.* **144** 118–41
[2] Andriollo T, Zhang Y, Faester S and Kouznetsova V 2020 Analysis of the correlation between micro-mechanical fields and fatigue crack propagation in nodular cast iron *Acta Mater.* **188** 302–314
[3] Verdu C, Adrien J and Buffière J Y 2008 Three-dimensional shape of the early stages of fatigue cracks nucleated in nodular cast iron *Mater. Sci. Eng. A* **483**–**484** 402–5
[4] Azeem M A, Bjerre M K, Atwood R C, Tiedje N and Lee P D 2018 Synchrotron quantification of graphite nodule evolution during the solidification of cast iron *Acta Mater.* **155** 393–401
[5] Buljac A, Helfen L, Hild F and Morgeneyer T F 2018 Effect of void arrangement on ductile damage mechanisms in nodular graphite cast iron: In situ 3D measurements *Eng. Fract. Mech.* **192** 242–61
[6] Limodin N, Réthoré J, Buffière J Y, Gravouil A, Hild F and Roux S 2009 Crack closure and stress intensity factor measurements in nodular graphite cast iron using three-dimensional correlation of laboratory X-ray microtomography images *Acta Mater.* **57** 4090–101
[7] Zhang Y B, Andriollo T, Fæster S, Barabash R, Xu R, Tiedje N, Thorborg J, Hattel J, Juul Jensen D and Hansen N 2019 Microstructure and residual elastic strain at graphite nodules in ductile cast iron analyzed by synchrotron X-ray microdiffraction *Acta Mater.* **167** 221–30
[8] Andriollo T, Hellström K, Sonne M R, Thorborg J, Tiedje N and Hattel J 2018 Uncovering the local inelastic interactions during manufacture of ductile cast iron: How the substructure of the graphite particles can induce residual stress concentrations in the matrix *J. Mech. Phys. Solids* **111** 333–57
[9] Freulon A, de Parseval P, Josse C, Bourdie J and Lacaze J 2016 Study of the Eutectoid Transformation in Nodular Cast Irons in Relation to Solidification Microsegregation *Metall. Mater. Trans. A Phys. Metall. Mater. Sci.* **47** 5362–71
[10] Abramowitz P and Moll R A 1970 Silicon-Carbon interaction and its effect on the notch toughness of mild steel *Metall. Trans.* **1** 1773–5
[11] Andriollo T, Zhang Y B, Fæster S, Thorborg J and Hattel J 2019 Impact of micro-scale residual stress on in-situ tensile testing of ductile cast iron: Digital volume correlation vs. model with fully resolved microstructure vs. periodic unit cell *J. Mech. Phys. Solids* **125** 714–35
[12] Thermo Scientific™ 2019 Avizo 9.6
[13] Bellini C, Di Cocco V, Favaro G, Iacoviello F and Sorrentino L 2019 Ductile cast irons: Microstructure influence on the fatigue initiation mechanisms *Fatigue Fract. Eng. Mater. Struct.* 1–11
[14] Andriollo T, Fæster S and Winther G 2018 Probing the structure and mechanical properties of the graphite nodules in ductile cast irons via nano-indentation *Mech. Mater.* **122** 85–95
[15] Matouš K, Geers M G D, Kouznetsova V G and Gillman A 2017 A review of predictive nonlinear theories for multiscale modeling of heterogeneous materials *J. Comput. Phys.* **330** 192–220
[16] Lacaze J 1999 Solidification of spheroidal graphite cast irons: III. Microsegregation related effects *Acta Mater.* **47** 3779–92
[17] Selig C and Lacaze A 2000 Study of microsegregation buildup during solidification of spheroidal graphite cast iron *Metall. Mater. Trans. B* **31** 827–36
[18] Boeri R and Weinberg F 1989 Microsegregation in Ductile Iron *AFS Trans.* **89** 179–84
[19] Xu C L, Andriollo T, Zhang Y B, Hernando J C, Hattel J and Tiedje N 2020 Micromechanical impact of solidification regions in ductile iron revealed via a 3D strain partitioning analysis method *Scr. Mater.* **178** 463–467.